UNIVERSITY OF LEEDS

This is a repository copy of *Incipient Slip Sensing for Improved Grasping in Robot Assisted Surgery*.

White Rose Research Online URL for this paper:
https://eprints.whiterose.ac.uk/188999/

Version: Accepted Version

Article:
Waters, I, Wang, L, Jones, D orcid.org/0000-0002-2961-8483 et al. (2 more authors) (2022) Incipient Slip Sensing for Improved Grasping in Robot Assisted Surgery. IEEE Sensors Journal, 22 (16). pp. 16545-16554. ISSN 1530-437X

https://doi.org/10.1109/jsen.2022.3187860

© 2022 IEEE. Personal use of this material is permitted. Permission from IEEE must be obtained for all other uses, in any current or future media, including reprinting/republishing this material for advertising or promotional purposes, creating new collective works, for resale or redistribution to servers or lists, or reuse of any copyrighted component of this work in other works.

Reuse
Items deposited in White Rose Research Online are protected by copyright, with all rights reserved unless indicated otherwise. They may be downloaded and/or printed for private study, or other acts as permitted by national copyright laws. The publisher or other rights holders may allow further reproduction and re-use of the full text version. This is indicated by the licence information on the White Rose Research Online record for the item.

Takedown
If you consider content in White Rose Research Online to be in breach of UK law, please notify us by emailing eprints@whiterose.ac.uk including the URL of the record and the reason for the withdrawal request.

White Rose university consortium
Universities of Leeds, Sheffield & York

eprints@whiterose.ac.uk
https://eprints.whiterose.ac.uk/

Incipient Slip Sensing for Improved Grasping in Robot Assisted Surgery

Ian Waters, Lefan Wang, Dominic Jones, Ali Alazmani, and Peter Culmer

***Abstract*— The limited grasping control available in Robot Assisted Surgery is considered a significant limitation of the technology. Traditionally the integration of haptic feedback has been proposed to resolve this issue but has found limited adoption. Here we investigate an alternate approach based on the concept of detecting localised slips caused by the intrinsic elastic properties of soft tissues. This method allows for the early detection of slip so that mitigating actions can be taken before gross slip can occur, allowing the grasper to minimise the force required to maintain stable grasp control. In this paper we detail the design of a sensor developed to detect incipient slip by monitoring the relative difference in tissue movement at the front and back of the grasper, caused by tissue slip. We then demonstrate the sensor's efficacy for the early detection of slip, as well as its ability to automate grasping under representative surgical conditions, with the automated case providing comparable performance to one which uses the maximum allowable grasp force. This work provides evidence that the slip detection methodology developed is consistently able to detect incipient slip before macro slip occurs, thus offering a strong basis for its use in automating surgical grasping tasks to avoid tissue trauma and slip.**

***Index Terms*— Medical, Surgical Robotics: Laparoscopy, Grasping, Slip sensor**

I. Introduction

ROBOTIC surgical devices have helped advance Minimally Invasive Surgery (MIS), with the introduction of 3D vision, tremor removal, and improved dexterity all contributing to improved surgical outcomes [1]. However the lack of haptic feedback is still highlighted as a major limitation of the technology [1], [2]. Robotic surgical devices mechanically separate the surgeon and patient, completely denuding the surgeon of their sense of touch, which is already significantly limited by the tools used in MIS procedures. This can lead to multiple issues including the over application of force, limited grasp control, tissue slip, and an inability to palpate tissue to identify abnormalities [3]–[5].

The use of haptic feedback during tissue grasping tasks has been demonstrated to reduce tissue trauma caused by crushing due to excessive grasping forces [6]–[8]. However it also increases the cognitive load on the surgeon, which could result in surgical errors [9], and there is a paucity of knowledge on its ability to prevent adverse slip events, which can delay surgery or lead to further complications [4]. We believe a more direct method of controlling the grasping force, whilst maintaining grip security, would be through slip monitoring and detection.

Paper was submitted for review on 08/01/2022

I. Waters, A. Alazmani and, P.Culmer are with the School of Mechanical Engineering, University of Leeds, UK. (e-mail: mn10iw@leeds.ac.uk, a.alazmani@leeds.ac.uk, p.r.culmer@leeds.ac.uk)

D. Jones is with the School of Electronic and Electrical Engineering, University of Leeds, UK. (e-mail: d.p.jones@leeds.ac.uk)

L. Wang was with the School of Mechanical Engineering, University of Leeds, UK. She is now with the Department of Engineering, University of Cambridge, UK. (e-mail: wanglfhit@gmail.com)

This work was supported by the Engineering and Physical Sciences Research Council (EPSRC) under grant EP/R513258/1 and supported by the National Institute for Health Research (NIHR). For the purpose of open access, the author(s) has applied a Creative Commons Attribution (CC BY) license to any Accepted Manuscript version arising.

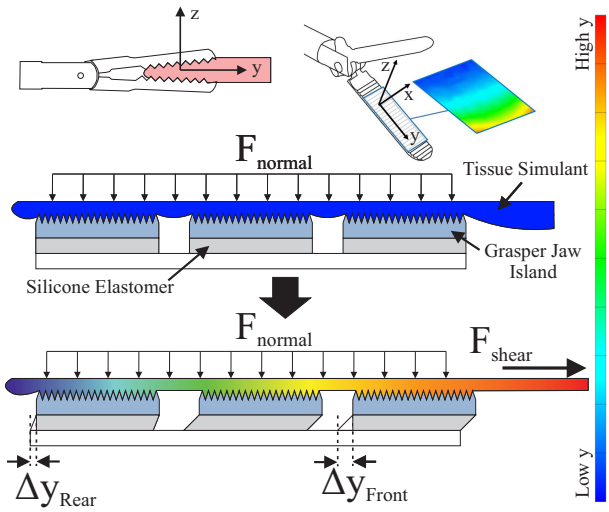

Fig. 1. Concept of the slip sensor's mechanical operation; the grasper face is separated into movable islands that can be tracked to detect the difference in slip between the front and rear of the grasper (The scale indicates the relative displacement of the colours used in the diagram).

If it is possible to detect the point in time when tissue starts to slip, then the gripping force can be adjusted to use the minimum force required to maintain stable control, reducing tissue trauma as well as the occurrence of slip events during surgery. This method of control also opens up the possibility for automation of grasping, allowing the surgeon to focus on more critical tasks [10].

Several notable examples of surgical graspers designed to detect slip have been reported. *Khadem et al.* [11] created a system that automatically adjusts the clamping load based on the applied retraction force, aiming to remain within a predefined safe grasping zone, however this requires prior knowledge of the slip behaviour of the grasped tissue. *Burkhard et*

al. [12] developed a method that aims to directly detect slip events, this uses a thermal sensing technology that monitors changes in heat flux through the tissue as it slips. This was able to detect slip after less than 2mm of gross tissue displacement in trials on porcine tissue. *Jones et al.* [13] developed a force based slip sensor, using a two axis soft inductive tactile sensor (SITS) to detect when the coefficient of friction first peaks during tissue retraction to indicate when slip has occurred. The common feature of the latter two approaches is that they aim to identify the time at which macro slip occurs, which requires the whole tissue contact area to be slipping before mitigating action can be taken, therefore risking a loss of grip stability. One possible solution to this is to focus on exploiting and sensing the occurrence of incipient slips.

Incipient slips are localised slips that occur prior to the onset of macro slip [14]. In incipient slip the total shear force is less than the total frictional force, but in localised areas of the surface contact the local shear force exceeds the local friction, causing small localised movements at the surface while the remainder of the contact remains static [14]. As more shear force is applied the number of incipient slip sites will increase, when the total shear force exceeds the total frictional force the entirety of the contact will begin to slip, otherwise termed macro slip [14].

The phenomenon of incipient slip helps human fingers detect slip before macro slips can occur [15], and has already been utilised by the wider robotics community to improve grasping [16], but currently has seen limited use in the field of surgical manipulation, or the grasping of deformable materials. *Stoll and Dupont* [17] looked to monitor changes in tissue stiffness as an indicator of incipient slip, but the method only measured global rather than local shear forces, and so would provide minimal time for mitigating actions to be taken.

The majority of incipient slip sensors developed by the wider robotics community use curved finger like surfaces to encourage incipient slip [16], [18], [19]. This curved surface results in a variation in the normal force across the surface, creating areas of high and low friction which lead to slips occurring preferentially towards the edge of the contact, where the normal force is low [16]. Despite using similar methods to encourage incipient slip a range of different sensing methods and modalities are used to detect it (e.g. vibration, shear force, normal force distribution and optical tracking), for a detailed summary of these see the review by *Chen et al.* [16]. We have previously produced an incipient slip sensor, for use with soft tissues, that utilises the variation of the normal force to induce predictable incipient slip events, which were monitored using a localised measurement system [20].

Our aim is to develop and evaluate an instrumented grasper face for detecting incipient slips before macro slip occurs. In section II we present the sensing concept and detailed design of the sensor system, before evaluating its efficacy over a range of operating conditions in Section III. A case study is then presented in Section IV to demonstrate the concept's feasibility for use in grasping automation. This work can then form the basis for a grasping system capable of automating grasping and force control within surgery, through the detection of incipient slip events.

II. System Development

A. Concept

The concept underpinning this work aims to exploit the deformable nature of soft tissue to create detectable levels of incipient slip. Although the majority of incipient slip sensors utilise variations in normal force to encourage incipient slip, they are generally attempting to grasp rigid objects [16], whereas many tissues in the human body are typically compliant and highly deformable. Therefore as tissue is retracted by a surgical grasper it stretches, creating a tensile force which is resisted by the friction at the grasper face. When the tensile shear force exceeds the frictional force the tissue at the front of the grasper will start to slip, allowing it to stretch and deform, causing the tensile force to then propagate along the grasper face to the adjacent section of tissue [21]. This leads to a propagation of slip, followed by tissue deformation, along the grasper face, resulting in a difference in the relative tissue displacement at the front and rear of the grasper (Fig. 1).

Our concept is based on monitoring the difference in local tissue displacement that occurs between the front and rear of the grasper, created by the propagation of slip along its length. To achieve this the grasper's surface is separated into multiple sections or 'islands' that can move independently of each other, similar to those we utilised previously [20]. As the tissue is retracted the tensile force applied to the front island causes it to move forward with the tissue, until the shear force acting between the tissue and island exceeds the frictional force, at which point the island's displacement will halt as the tissue slips. The tension will then propagate through to the next island, as the front island is no longer maintaining a secure grip, resulting in the occurrence of displacement and then slip at each subsequent island (Fig 1). Consequently by tracking the displacement of the islands it is possible to detect when the tissue first slips against the front island, whilst the other islands maintain a stable control of the tissue. The novelty of this sensor system is the way in which it harnesses the deformation inherent in soft tissues to create measurable levels of incipient slip, which can be detected before the onset of macro slip.

B. System Design and Fabrication

A scaled demonstration of a surgical grasper (Fig. 2) was developed to evaluate this concept. This consists of three islands distributed along the length of the grasper that can move independently of each other, with sensors positioned beneath the front and rear island to track their displacement. Each island consists of a 3D printed rigid gripping surface (Rigid 4000 Resin, Formlabs), with a 1 mm layer of silicone elastomer (Ecoflex 00-30, Smooth-on) underneath to allow them to move freely. The grasper was scaled up from a standard surgical grasper to allow for improved characterisation and analysis of incipient slip, and its associated mechanics. A regular hexagonal pattern (0.75 mm height, width and separation) was applied to the surface of the grasper as this provides isometric frictional properties, which can easily be varied through altering the pattern density [21], [22].

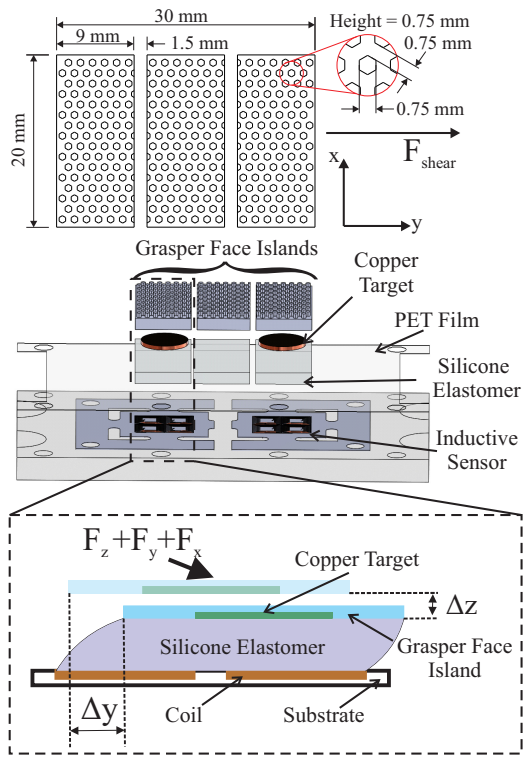

Fig. 2. Top: Dimensioned grasper face islands. Middle: Exploded model of the different components making up the sensor system. Bottom: Illustration of principal of operation of SITS sensors.

To monitor the relative displacement of the islands tri-axis SITS sensors were selected due to their thin form factor, and the ability to tune their resolution to suite the desired application [23], [24]. These utilise the eddy current effect to detect the movement of a conductive target over a set of sensing coils. Eddy currents are induced within the conductive target by an alternating current passing through the coils, in turn this produces a magnetic field which opposes the original field of the coils, causing a change in their inductance (Fig.2). The variation of this inductance across a set of four coils can then be used to determine the position and movement of the target above them [23].

The SITS sensors utilised consisted of four 5mm square coils each consisting of 3 layers of coils with a 0.1 mm pitch, a 0.1 mm trace width, with 10 turns per layer, whilst a copper disc (8 mm diameter $\times$ 0.8mm) embedded in the base of the rigid gripping surface was used as the conductive target. A 0.15 mm layer of PET film was placed above the coils to protect them from any fluid ingress (Fig. 2). To measure their change in inductance a four channel inductance to digital converter chip was used (LDC1614, Texas Instruments). For more information on the design and operation of these sensors see [23], [24]. The sensors were monitored and controlled via a microcontroller (Teensy 3.6, PJRC) using the I^2C serial protocol.

C. Data Processing

To calibrate the SITS sensors a multi axis sensor calibration rig was employed [24], this moves the conductive target over each set of four coils using three linear stages, monitoring

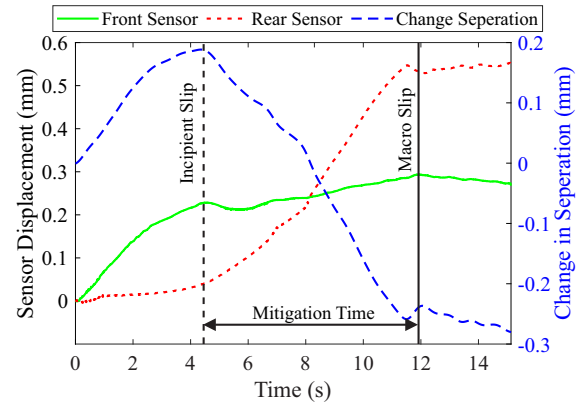

Fig. 3. Example trace showing the displacement of the front and rear senor islands, as well as the change in the separation between the two. Test conditions: Mat A, 20 N clamp load, and 2 mm/s retraction speed.

its displacement in x,y and z via a set of encoders. A 3D scanning operation was carried out with z stepped in 0.2 mm increments from z=-0.6:1.2 mm, and a grid scan conducted between y=-3:3 mm and x=-1:1 mm at each z level, where {0,0,0} represents the position of the target in its unloaded 'neutral' position.

A neural network was implemented to determine the sensor displacement (D) from the inductance values (I) of the four coils,

$$D_{x,y,z} = f(I_{1,2,3,4}) \tag{1}$$

using the Matlab neural net fitting toolbox (Matlab, Mathworks). The neural net consisted of a two-layer feed forward neural network with 15 neurons in the hidden layer, with the Tanh function used as the activation function, and the Levenberg-Marquardt back propagation algorithm as the training method, these were selected based on prior research [24]. Validation of this model against a separate data set showed a high correlation with the output of the neural net, with root mean squared errors of 0.043 mm, 0.050 mm and 0.064 mm, in x, y and z respectively.

D. Slip Detection

In the context of this paper incipient slip refers to the condition when at least one of the islands is found to be slipping against the tissue, while the remaining islands retain a stable grip. With the current sensor design the whole of the island's contact area must be slipping against the tissue for slip to be detectable at that island. During retraction this will always occur at the front islands first due to the way shear forces, and the resultant slip, propagate from the front to rear of the grasper, as detailed in Section II-A.

To be able to identify the time at which incipient slip starts to occur at the front sensor an algorithm was developed using initial trial data (See Fig. 5), an example trace is shown in Figure 3. This algorithm was focused on detecting slip during grasper retraction as this is considered the most challenging case, when tissue is most likely to slip during surgery due to the higher shear forces being applied.

From Figure 3 it can be observed that an incipient slip event occurs at the front island around the 4 second mark, indicated

by the plateauing of the displacement, suggesting the island is no longer moving with the retracting tissue. As the front sensor begins to slip the rear sensor then starts to take up tension, indicated by its rapid increase in displacement after the incipient slip event occurs at the front island, as the tension, deformation, and slip propagate from the front to the back of the grasper.

By calculating the change in the separation between the front and rear islands, as shown in Figure 3, a clear peak appears when the front island starts to slip against the tissue. This peak occurs because as the front island starts to slip, the rear islands start to take up tension (due to the slip propagation along the grasper), thus reducing the separation between the front and rear islands after this point. To automatically identify the time at which this peak occurs, and therefore incipient slip, the differential of the change in separation between the two sensors was defined as,

$$S = \frac{d(\Delta y_{Front} - \Delta y_{Rear})}{dt} \tag{2}$$

where S is the rate of change in separation, and y is the displacement in the direction of shear of the front and rear sensors. A third order Butterworth filter with a cut off frequency of 5 Hz was then applied to attenuate noise. When the mean value of the rate of change of separation measured over a 0.1 s period first becomes less than 0, indicating a peak, incipient slip of the front island is considered to have occurred, where $t = n$ is the current time. This algorithm was developed at a sample rate of 100 Hz.

$$\overline{[S]}_{t=n-0.1}^{t=n} < 0 \tag{3}$$

III. System Evaluation

To evaluate the performance of the sensor to identify incipient slip prior to macro slip a test rig was developed, this simulates the clamping and retraction of tissue under representative surgical conditions. A typical test involved clamping the tissue between the sensored grasper face and a flat surface, at a constant fixed load, before retracting the tissue in a direction parallel to the grasper face along its length for 30 mm, to ensure that the tissue enters the macro slip regime.

A. Experimental Set up and Analysis

An adaption of the test rig from [21] was used to create a controlled simulation of surgical grasping and retraction (Fig. 4). This consists of a linear load tester (Instron 5940, Instron) for tissue retraction, and a pneumatic piston (MGPM20TF-75Z, SMC) & (ITV1030,SMC) regulator to simulate grasping under a constant load. The retraction distance and global shear force were logged via the linear load tester, whilst the SITS sensors were monitored via the microcontroller. All data logging and control was managed and synchronised between the linear load tester and the microcontroller using a real-time embedded control board (MyRIO, National Instruments), with a sample rate of 100 Hz. Tissue simulants were clamped against a clear acrylic plate with a camera (AVE2, Instron) positioned behind it, this captured images at a rate of 50 Hz

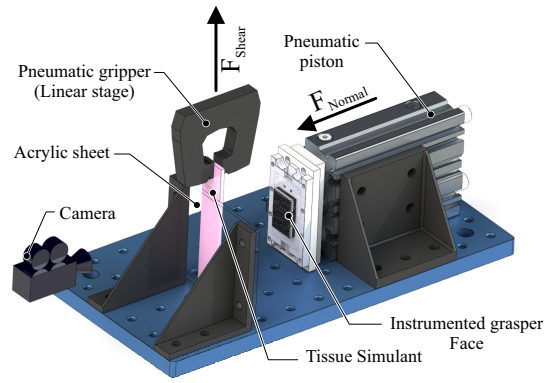

Fig. 4. Model of the testing setup used for simulating the clamping and retraction of tissue.

for use in tracking the displacement of the tissue simulant through Digital Image Correlation (DIC).

B. Data Analysis

The time macro slip occurs can be identified by monitoring when the global shear force acting on the tissue starts to plateau, as this indicates the tissue is fully slipping against the grasper, preventing further increases in the tensile force of the tissue. To calculate the time of macro slip the differential of the global shear force (F_S), measured by the linear load tester, was used to identify when the shear force starts to level off.

$$\overline{\left[\frac{dF_S}{dt}\right]}_{t=n-0.1}^{t=n} < 0.025V_s, \tag{4}$$

When the rate of change of force, averaged over the previous 0.1 s, is less than 0.025 times the retraction speed (V_s), macro slip is indicated to have occurred.

The time difference between the point of macro slip and the point that incipient slip is detected was then calculated, this gives an indication of the available time to take mitigating action, termed the mitigation time (Fig. 3).

For validation of the actual magnitude of displacement and slip that is occurring between the tissue simulant and grasper face, the displacement of the tissue simulant was tracked using images from the camera and DIC software (GOM Correlate, GOM). The average displacement of the tissue grasped by the the front, central, and rear grasper islands during the initial clamping action was tracked throughout the retraction, in the direction of shear.

C. Experimental Parameters

To analyse the sensor characteristics a set of operating parameters were defined based on those use in typical surgical practice. The major variables identified were the clamping force, retraction speed, and material stiffness.

A clamping force range of 10-30 N was selected as this approximates the applied pressure range of a standard surgical grasper [25], [26], and a retraction speed range of 1-5 mm/s was used, based on standard laparoscopic retraction speeds for tissue manipulation and grasper retraction [27].

Due to the inherent variability with using biological tissue samples a range of tissue simulants were developed to vary the

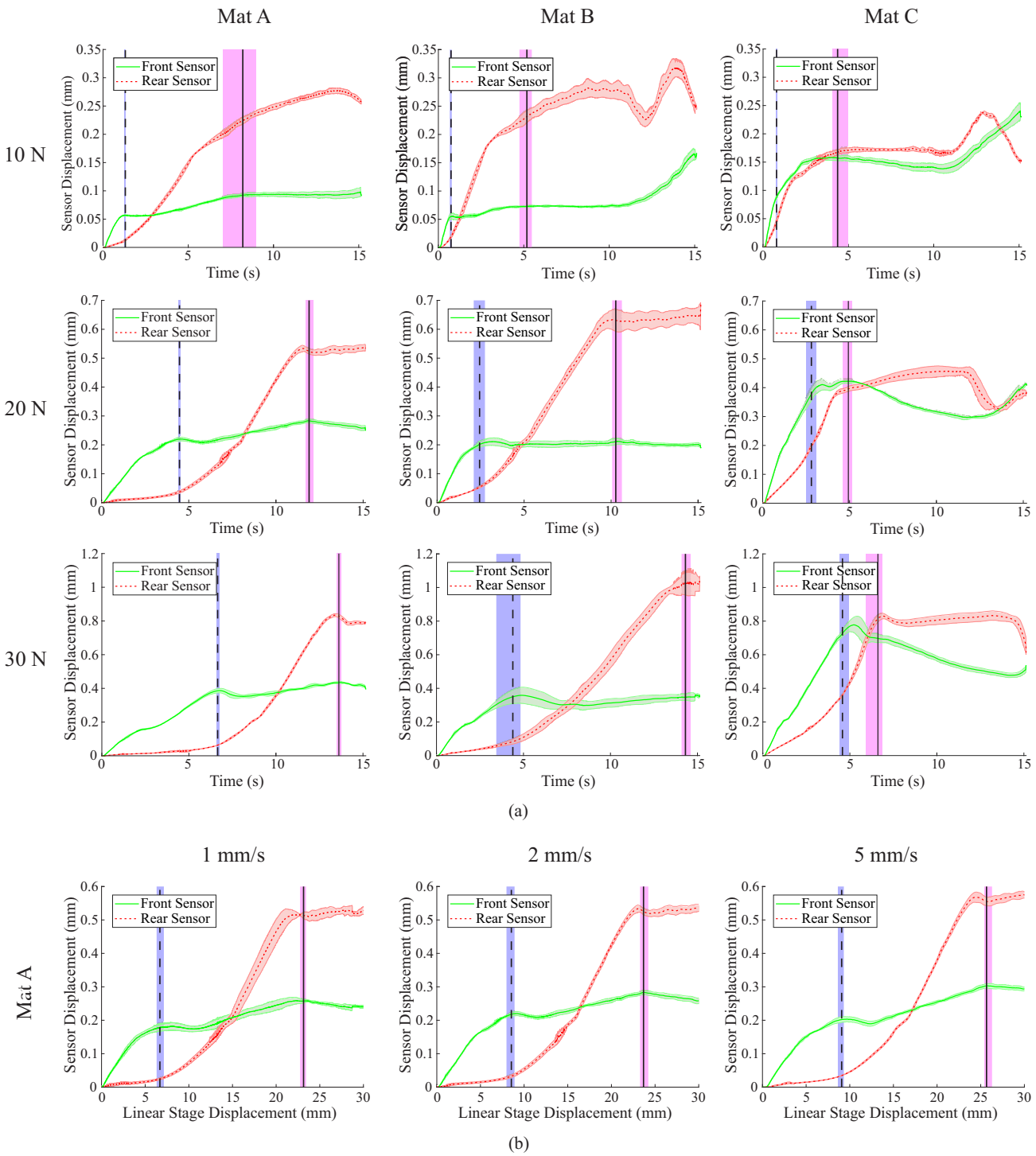

Fig. 5. Graphs showing average sensor displacement, with the shaded area representing the standard deviation. The vertical dotted lines indicates the time incipient slip occurs, while the solid vertical line indicates the time of macro slip, the shaded areas around each show range of slip times/displacements. a) Sensor displacement vs time for changes in force and material stiffness at a retraction speed of 2 mm/s. b) Sensor displacement vs linear stage displacement (retraction distance) for variations in retractions speed for Mat A under a 20 N clamping load.

material stiffness in a more repeatable manner. Three different tissue simulants were created that mimic the tensile properties of liver tissue [28]. The simulants consist of 3 layers of silicone elastomer (Ecoflex 00-30, Smooth-on) with different fabrics sandwiched between each layer of silicone to vary the elastic modulus (E), whilst maintaining similar frictional and compressive properties. Material A (Mat A - E = 241 kPa) and B (Mat B - E = 320 kPa) used 2 & 4 layers of a lightweight netted spandex respectively, whilst Material C (Mat C - E = 610 kPa) used 2 layers of a higher density woven spandex. These simulants were fabricated using the silicone applicator from [29] to form a 3 mm thick sample, with the fabric layers placed 0.3 mm below each surface, these were then laser cut into 20 mm x 100 mm strips. To allow tissue displacements to be tracked using DIC a speckle pattern was applied to one side using enamel spray paint, with a very thin 0.05 mm layer of

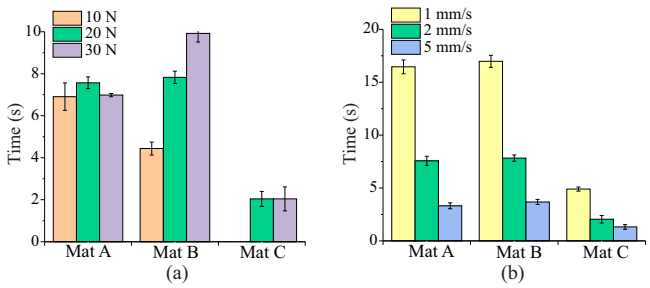

Fig. 6. Graphs showing the mean time difference between the detection of incipient and macro slip (N=5), the error bars indicate the standard deviation. (a) Variation of force and material stiffness at 2 mm/s retraction speed. (b) Variation of speed and material stiffness at 20 N clamp load.

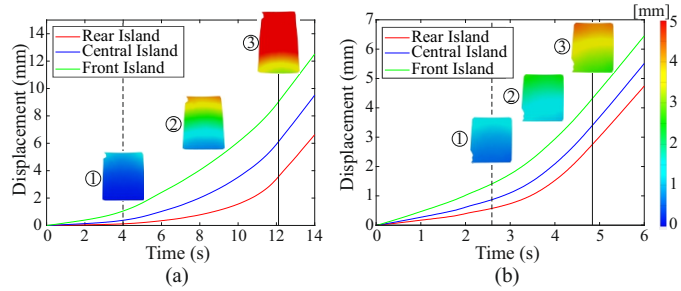

Fig. 7. Graphs show the average tissue displacement at the front, central and rear islands measured using DIC. The dotted line indicates the point of incipient slip while the solid line indicates macro slip. Colour maps show displacement profiles, 1 is the point of incipient slip, 2 is midway between incipient and macro slip, and 3 is the point of macro slip (a) Mat A, 20 N, 2 mm/s. (b) Mat C, 20 N, 2 mm/s.

silicone applied on top to prevent delamination of the pattern. A layer of surfactant lubricant was applied to the surface of the simulants before each test, simulating the serous fluid that coats most organs [30]. To calculate the elastic modulus of the three different simulants ATSM D412 Type C tensile specimens were evaluated on a linear load tester.

D. Results

Figure 5 (a) provides a summary of the average displacement measured by the sensors under the front and rear islands, for variations in the material stiffness and clamping force. Early signs of incipient slip are identifiable in the majority of cases, indicated by the plateauing of the front sensor's displacement, followed by a rapid increase in the displacement of the rear sensor island. The exception to this is the 10 N load case for the high stiffness material, Mat C, where both front and rear take up tension and then slip almost simultaneously.

The results for the influence of varying retraction speed on sensor displacements are shown in Figure 5 (b), these are plotted against the displacement of the linear stage to normalise the x axis scale for the different retraction speeds. In all test cases the front island clearly slips before the rear island, allowing for reliable early detection of incipient slip. Despite large variations in the retraction speed, the retraction distance at which incipient and macro slip occur shows minimal change.

A summary of the effects of the clamp force, material stiffness and retraction speed on the available mitigation time are provided in Figure 6. In all cases where incipient slip is reliably detected there is at least a 1.3 s gap between incipient slip detection and the occurrence of macro slip. Retraction speed was found to be inversely proportional to the mitigation time, with a doubling of retraction speed resulting in a 55% reduction in the available time. The variation in force appeared to have no significant effect on mitigation time (once incipient slip was detectable) for Mat A & C, however, for Mat B increases in clamp load resulted in significant increases in mitigation time. Material stiffness had the most significant effect on mitigation time, comparing Mat A and Mat C (to exclude influence of force in Mat B), a 2.5 times increase in the material stiffness from Mat A to Mat C results in a 73% reduction in the available mitigation time for the 20 N load case and a 71% reduction in the 30 N case.

The tissue displacement characteristics measured using the DIC system are presented in Figure 7. These show how the average tissue displacement under the islands varies over time for both Mat A and Mat C. Data is shown from the start of retraction until macro slip has occurred. In addition, the spatial displacement distribution across the grasper face at key time points is shown as a series of colour maps.

During the early stages of retraction there is a gradual increase in tissue displacement at the front of the grasper, whilst towards the rear the tissue motion is significantly lower. As the retraction progresses, slip propagates along the length of the grasper, leading to increases in the magnitude and rate of tissue displacement under successive grasper islands. This continues until the point of macro slip, when the full contact area of the grasper begins to slip, after which all three islands move at the speed of retraction. For the low stiffness material (Mat A) this process of slip propagation is gradual, with the front tissue showing significant displacement (and so slip) before movement is observed at the rear of the grasper. The stiffer tissue (Mat C) displays more rapid slip propagation, with tissue displacement evident at the rear of the grasper by the time that incipient slip is detected at the front island. Comparing these responses at the point of incipient slip, the tissue at the rear of the grasper has moved 0.12 mm and 0.60 mm for Mat A and C respectively, whilst the front had displaced 1.05 mm (Mat A) and 1.46 mm (Mat C), clearly highlighting how a slip differential develops along the length of the grasper face during retraction.

IV. Case Study: Automation

To investigate the efficacy of using the presented incipient slip detection technique for automating grasping a case study was conducted. A simple algorithm was created that applies an initial clamping load of 10 N, and then scans for incipient slip event using the algorithm detailed in Section II. When incipient slip is detected the clamp force is increased by 5 N, the system then pauses for 1 s to allow the clamp force to be applied, and then starts the scan operation again, it carries on stepping the force up to a maximum of 30 N. The maximum and minimum force used were based on those from the previous set of tests, while the 5 N step was selected to ensure that propagation of the slip front is prevented by the step increase, whilst still providing a range of graduations between the maximum and minimum force.

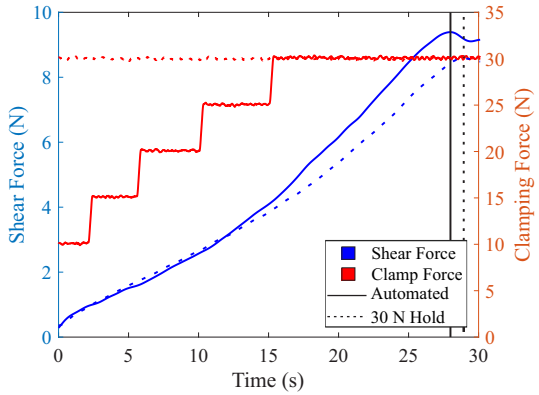

Fig. 8. Variation in shear and clamp loads for automated and fixed load control methods. The black vertical lines indicate the times of macro slip for each case. Mat A with a 1 mm/s retraction speed.

The analysis was carried out with a retraction speed of 1 mm/s using Mat A as the tissue simulant. These parameters were selected as they provide a large time window for mitigating action to be taken, and allow for a consistent and repeatable detection of incipient slip, events even at low forces, providing optimal conditions for successful slip detection and mitigation. To assess the capability of the automated slip mitigation system it was compared to a case in which a fixed 30 N clamping load was applied throughout the retraction, to evaluate its performance against the maximum clamp load scenario.

The variation in shear force over time in the automated and 30 N load cases show a strong correlation with each other, despite the large differences in the clamping load being applied throughout the retraction (Fig. 8). Both control methods also produced a similar time to macro slip, with a time of 27.90±0.1 s for the automated case and 29.26±0.24 s for the constant 30 N load case. They also required similar shear loads to induce macro slip, with peak loads of 9.64±0.15 N and 8.84±0.21 N, for the automated and constant 30 N load cases respectively.

To provide an indicator of the potential for tissue damage to occur, as a result of grasping, the applied impulse was calculated, as both the magnitude of force and the time over which it is applied have an influence on the level of tissue trauma observed [31]. The impulse was calculated by integrating the clamp force over time up to the point of macro slip. The 30 N load case exhibited an average impulse of 879.18±7.46 N.s, while the automated control method exhibited approximately 23% less impulse at 677.8±3.5 N.s.

The results for the tissue displacement observed using DIC (Fig. 9(a)) indicate that there is more tissue displacement at the front of the grasper in the automated case, as the tissue slips against the sensor, with up to 1.5 mm more displacement than in the fixed 30 N load case. However, the displacements of the central and rear islands maintain a much higher correlation between the two control methods throughout the full retraction. Some of the additional displacement observed at the front is the result of tissue compression during the step changes in clamp load, rather than the tissue slip, this is indicated by the step change in displacement at the points that the step change in clamp load occurs (Fig. 9(a)). The colour maps in Figure

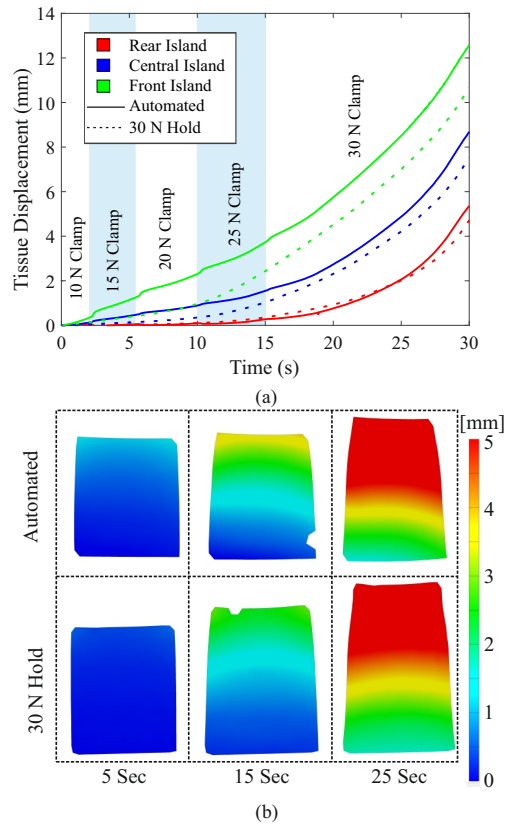

Fig. 9. Comparison of tissue displacement for automated and fixed load control methods. Test carried out on Mat A with a 1 mm/s retraction speed. (a) Average displacement of tissue under the front, central and rear islands. (b) Colour map showing tissue displacements.

9(b) show a similar pattern, with the tissue slip and subsequent displacement propagating slightly faster in the automated test case.

V. Discussion

This work demonstrates that by utilising the deformable nature of the grasped material, it is possible to reliably encourage detectable levels of preferential incipient slip in deformable materials, that are similar to biological tissue. The grasper and sensor system developed were able to sense the onset and progression of incipient slip under a range of representative surgical conditions, with a sufficient time window for mitigating actions to be implemented before macro slip occurs.

The sensor technology and associated slip detection algorithm showed high reliability when grasping lower stiffness materials (Mat A & B), accurately identifying when incipient slip occurs at the front island, across the full range of clamp forces (Fig. 5). For the high stiffness material (Mat C) the system was able to detect incipient slip consistently in the higher clamp load cases, however for the 10 N case the algorithm produced a false positive, indicating incipient slip had occurred after approximately 1 s, even though displacement of the front sensor had not started to plateau. In this case the front and rear sensor take up tension and then slip almost simultaneously, rather than the gradual propagation from the front to rear of the grasper observed in the other cases. This is

because the tissue behaviour tends towards rigid body motion as the stiffness increases, so slip propagates more rapidly from the front to rear, acting on each sensor island almost simultaneously. Similar behaviour can also be observed for the high stiffness 20 N & 30 N load cases, where there is significantly less delay between the front and rear islands taking up tension compared to the lower stiffness materials, however the slip prorogation is still slow enough for incipient slip to be reliably detected (Fig 5).

Despite low forces making the detection of incipient slip challenging, once it becomes possible to detect incipient slip, further increases in clamp load didn't significantly affect the available mitigation time, for either Mat A or C (Fig. 6). This is because the increase in clamping force delayed the occurrence of both incipient and macro slip by a similar amount, maintaining a similar mitigation time (Fig. 5). However Mat B appears to react differently to changes in clamp load, with increases in force providing progressive increases in the available mitigation time (Fig. 6). The point at which incipient slip is first detected increases by a similar magnitude to Mat A for each step increase in clamp force, but the point of macro slip is much more delayed (Fig. 5). Further investigation is required to understand the cause of this behaviour.

Variations in the material stiffness also significantly affected the available mitigation time. This was particularly evident for the high stiffness material, Mat C, its increased stiffness caused a significant decrease in the available time (Fig 6). As stated earlier this is due to the transition towards more rigid behaviour, with the slip propagating through the material much quicker, significantly reducing the time at which macro slip occurs, and resulting in minimal delay between slip at the front and rear islands (Fig. 5).

The variation of retraction speed had minimal affect on the ability of the system to detect incipient slip (Fig. 5), but a significant effect on the available mitigation time (Fig. 6). This is because variations in the retraction speed don't affect the shape or amplitude of the sensor displacement curves, but instead scales them along the time axis, as shown when plotting them against the linear stage displacement (Fig. 5). The points of incipient and macro slip occur at approximately the same linear displacement for all 3 retraction speeds, whilst the mitigation time scales inversely with retraction speed, with a doubling in retraction speed resulting in approximately half the available mitigation time.

The displacement characteristics of the islands as measured by the sensors (see Fig. 5) correlate with those measured by the DIC system up to the point incipient slip is detected. The absolute magnitude of displacement differs between the measures because the DIC reports the average displacement of the tissue under the whole island, whereas the sensor movement is dependent on the tissue movement at the rear of the island (the last contact point to slip).However, the overall characteristics show agreement and support the premise on which this technique is based, that tissue propagation occurs progressively from the front to the rear of the grasper during retraction.

The case study into the automation of the grasping action further demonstrates the efficacy of the methodology and system developed for the early detection of tissue slip, and demonstrates that it could be an effective means of automating the grasp control, and reducing the applied gripping force, helping to reduce tissue trauma. The automated control system was able to detect the occurrence of tissue slip at the front island, and increased the clamp load to prevent it, limiting the rate of slip propagation to a similar level observed for the max load case (Fig. 9). This resulted in comparable grasping performance, with similar times till macro slip, and similar peak shear forces required to induce it, whilst reducing the impulse and applied clamp forces during the earlier stages of retraction (Fig 8), limiting the probability of tissue trauma [31].

Several factors were identified within this laboratory-based work that require further investigation, prior to translation into surgical practice, since they may introduce uncertainties which effect the performance of this technique:

- Size: the current prototype is scaled-up and would need a 50-100% reduction in size to meet the size of typical robotic surgical graspers. The magnitude of this scale change is unlikely to impact on the incipient slip mechanics between tissue and grasper which are central to this sensor. However, it will be significantly more challenging to construct an instrumented multi-island grasper face at this scale, without recourse to alternative manufacturing techniques, an area of ongoing research.
- Tissue properties: the incipient slip sensing method presented here does not require knowledge of the mechanical properties of a grasped tissue to detect slip. However, mechanical factors that effect the rate of slip propagation across the grasper face will determine the sensitivity of the system and its ability to act as a slip 'early-warning' system. In addition, biological tissues exhibit significant heterogeneity in comparison to the simulants presented here. Accordingly, it will be important to evaluate a range of biological tissues to determine appropriate operating regimes in both mechanical terms (e.g. stiffness, lubrication regime, viscoelasticity) and the clinical focus (e.g. tissue types).
- Surgical use: in this study, surgical grasping was simplified as controlled uniaxial retraction between parallel grasper faces. In reality, surgical manipulation is more complex, involving additional lateral motion and rotation of the grasper, together with pivoted 'scissor action' jaws. Determining the impact of these factors on slip-sensing performance will require additional study focused on grasper kinematics.
- Automation: in this study, the algorithm used to automate grasping operates in isolation. Translation towards surgical use will require integration of these aspects into the control scheme of the surgical robot. This has the opportunity to enhance the slip detection and prevention algorithm, by providing it with additional contextual information from the robot system (e.g. grasper position, speed, and visual cues). Ultimately, while the progression of autonomy in surgical robotics must be pursued with caution, enhanced grasping control has the potential to

operate transparently to the surgeon, in a similar fashion to anti-lock braking systems that are now a common and invaluable feature of the modern car.

VI. Conclusions and Further Work

In summary, the slip detection methodology, and associated sensing system, detailed in this paper are capable of providing significant improvements in the early detection of incipient slip when grasping deformable materials, well before macro slip occurs. This allows for mitigating actions to be taken automatically to prevent slip events, and maintain stable control of the tissue, whilst reducing the applied grasping forces. However, this method of slip detection is limited to applications involving softer more deformable materials, as higher stiffness materials produce less clear slip differentials between the front and rear of the grasper, especially in low force cases due to the high rate of slip propagation.

Further work is now required to fully understand the range of biological tissues for which this method would be suitable. In addition work is required on developing the sensing technology utilised to miniaturise it so that it can be suitably integrated within a standard surgical grasper. However, this body of work provides strong evidence that the developed sensing methodology is capable of providing significant improvements towards the automation of slip detection and force control in surgical robotics, minimising the occurrence of tissue trauma and adverse tissue slip events.

References

[1] D. M. Herron and M. Marohn, "Prepared by the SAGES-MIRA Robotic Surgery Consensus Group," p. 24, 2006.

[2] O. A. J. van der Meijden and M. P. Schijven, "The value of haptic feedback in conventional and robot-assisted minimal invasive surgery and virtual reality training: a current review," *Surgical Endoscopy*, vol. 23, no. 6, pp. 1180–1190, Jun. 2009.

[3] G. Tholey, J. P. Desai, and A. E. Castellanos, "Force Feedback Plays a Significant Role in Minimally Invasive Surgery," *Annals of Surgery*, vol. 241, no. 1, p. 8, 2005.

[4] B. Tang, G. Hanna, and A. Cuschieri, "Analysis of errors enacted by surgical trainees during skills training courses," *Surgery*, vol. 138, no. 1, pp. 14–20, Jul. 2005.

[5] E. Heijnsdijk, J. Dankelman, and D. Gouma, "Effectiveness of grasping and duration of clamping using laparoscopic graspers," *Surgical Endoscopy*, vol. 16, no. 9, pp. 1329–1331, Sep. 2002.

[6] C.-H. King, M. Culjat, M. Franco, C. Lewis, E. Dutson, W. Grundfest, and J. Bisley, "Tactile Feedback Induces Reduced Grasping Force in Robot-Assisted Surgery," *IEEE Transactions on Haptics*, vol. 2, no. 2, pp. 103–110, Apr. 2009.

[7] C.-H. King, M. Culjat, M. Franco, J. Bisley, G. Carman, E. Dutson, and W. Grundfest, "A Multielement Tactile Feedback System for Robot-Assisted Minimally Invasive Surgery," *IEEE Transactions on Haptics*, vol. 2, no. 1, pp. 52–56, Jan. 2009.

[8] V. Nitsch and B. Farber, "A Meta-Analysis of the Effects of Haptic Interfaces on Task Performance with Teleoperation Systems," *IEEE Transactions on Haptics*, vol. 6, no. 4, pp. 387–398, Oct. 2013.

[9] N. T. Burkhard, J. Ryan Steger, and M. R. Cutkosky, "The Role of Tissue Slip Feedback in Robot-Assisted Surgery," *Journal of Medical Devices*, vol. 13, no. 2, p. 021003, Jun. 2019.

[10] G.-Z. Yang, J. Cambias, K. Cleary, E. Daimler, J. Drake, P. E. Dupont, N. Hata, P. Kazanzides, S. Martel, R. V. Patel, V. J. Santos, and R. H. Taylor, "Medical robotics—Regulatory, ethical, and legal considerations for increasing levels of autonomy," *Science Robotics*, vol. 2, no. 4, p. eaam8638, Mar. 2017.

[11] S. M. Khadem, S. Behzadipour, A. Mirbagheri, and F. Farahmand, "A modular force-controlled robotic instrument for minimally invasive surgery - efficacy for being used in autonomous grasping against a variable pull force: Modular force-controlled robotic instrument," *The International Journal of Medical Robotics and Computer Assisted Surgery*, vol. 12, no. 4, pp. 620–633, Dec. 2016.

[12] N. T. Burkhard, M. R. Cutkosky, and J. R. Steger, "Slip Sensing for Intelligent, Improved Grasping and Retraction in Robot-Assisted Surgery," *IEEE Robotics and Automation Letters*, vol. 3, no. 4, pp. 4148–4155, Oct. 2018.

[13] D. Jones, A. Alazmani, and P. Culmer, "A Soft Inductive Tactile Sensor for Slip Detection Within a Surgical Grasper Jaw," p. 4, 2019.

[14] K. L. Johnson, *Contact mechanics*. Cambridge Cambridgeshire New York: Cambridge University Press, 1987.

[15] B. Delhaye, P. Lefevre, and J.-L. Thonnard, "Dynamics of fingertip contact during the onset of tangential slip," *Journal of The Royal Society Interface*, vol. 11, no. 100, pp. 20 140 698–20 140 698, Sep. 2014.

[16] W. Chen, H. Khamis, I. Birznieks, N. F. Lepora, and S. J. Redmond, "Tactile Sensors for Friction Estimation and Incipient Slip Detection – Towards Dexterous Robotic Manipulation: A Review," *IEEE Sensors Journal*, pp. 1–1, 2018.

[17] J. Stoll and P. Dupont, "Force Control for Grasping Soft Tissue," p. 4, May 2006.

[18] M. Tremblay and M. Cutkosky, "Estimating friction using incipient slip sensing during a manipulation task," in *[1993] Proceedings IEEE International Conference on Robotics and Automation*. Atlanta, GA, USA: IEEE Comput. Soc. Press, 1993, pp. 429–434.

[19] F. Veiga, J. Peters, and T. Hermans, "Grip Stabilization of Novel Objects using Slip Prediction," *IEEE Transactions on Haptics*, pp. 1–1, 2018.

[20] I. Waters, D. Jones, A. Alazmani, and P. R. Culmer, "Utilising Incipient Slip for Grasping Automation in Robot Assisted Surgery," *IEEE Robotics and Automation Letters*, vol. 7, no. 2, pp. 1071–1078, Apr. 2022.

[21] I. Waters, A. Alazmani, and P. Culmer, "Engineering incipient slip into surgical graspers to enhance grasp performance," *IEEE Transactions on Medical Robotics and Bionics*, pp. 1–1, 2020.

[22] J. C. Norton, J. H. Boyle, A. Alazmani, P. R. Culmer, and A. Neville, "Macro-Scale Tread Patterns for Traction in the Intestine," *IEEE Transactions on Biomedical Engineering*, vol. 67, no. 11, pp. 3262–3273, Nov. 2020.

[23] H. Wang, D. Jones, G. de Boer, J. Kow, L. Beccai, A. Alazmani, and P. Culmer, "Design and Characterization of Tri-Axis Soft Inductive Tactile Sensors," *IEEE Sensors Journal*, vol. 18, no. 19, pp. 7793–7801, Oct. 2018.

[24] L. Wang, D. Jones, G. J. Chapman, H. J. Siddle, D. A. Russell, A. Alazmani, and P. Culmer, "An Inductive Force Sensor for In-Shoe Plantar Normal and Shear Load Measurement," *IEEE Sensors Journal*, pp. 1–1, 2020.

[25] A. W. Brown, S. I. Brown, D. Mclean, Z. Wang, and A. Cuschieri, "Impact of fenestrations and surface profiling on the holding of tissue by parallel occlusion laparoscopic graspers," *Surgical Endoscopy*, vol. 28, no. 4, pp. 1277–1283, Apr. 2014.

[26] P. Mucksavage, D. C. Kerbl, D. L. Pick, J. Y. Lee, E. M. McDougall, and M. K. Louie, "Differences in Grip Forces Among Various Robotic Instruments and da Vinci Surgical Platforms," *Journal of Endourology*, vol. 25, no. 3, pp. 523–528, Mar. 2011.

[27] A. Alazmani, R. Roshan, D. G. Jayne, A. Neville, and P. Culmer, "Friction characteristics of trocars in laparoscopic surgery," *Proceedings of the Institution of Mechanical Engineers, Part H: Journal of Engineering in Medicine*, vol. 229, no. 4, pp. 271–279, Apr. 2015.

[28] A. R. Kemper, A. C. Santago, J. D. Stitzel, J. L. Sparks, and S. M. Duma, "Biomechanical Response of Human Liver in Tensile Loading," p. 12, Jan. 2010.

[29] J. W. Kow, P. Culmer, and A. Alazmani, "Thin soft layered actuator based on a novel fabrication technique," in *2018 IEEE International Conference on Soft Robotics (RoboSoft)*. Livorno: IEEE, Apr. 2018, pp. 176–181.

[30] W. Schwarz, "The surface film on the mesothelium of the serous membranes of the rat," *Zeitschrift fr Zellforschung und mikroskopische Anatomie*, vol. 147, no. 4, pp. 595–597, 1974.

[31] A. I. Margovsky, R. S. A. Lord, and A. J. Chambers, "The effect of arterial clamp duration on endothelial injury: An experimental study," *ANZ Journal of Surgery*, vol. 67, no. 7, pp. 448–451, Jul. 1997.